Dental Materials Journal 2020; 39(2): 287–294

Comparative biological assessments of endodontic root canal sealer containing surface pre-reacted glass-ionomer (S-PRG) filler or silica filler

Hirofumi MIYAJI[1,2], Kayoko MAYUMI[2], Saori MIYATA[1], Erika NISHIDA[1], Kanako SHITOMI[2], Asako HAMAMOTO[2], Saori TANAKA[2,3] and Tsukasa AKASAKA[4]

[1] *Clinic of Endodontics and Periodontics, Hokkaido University Hospital, N14 W5, Kita-ku, Sapporo, Hokkaido 060-8648, Japan*
[2] *Department of Periodontology and Endodontology, Faculty of Dental Medicine, Hokkaido University, N13 W7, Kita-ku, Sapporo, Hokkaido 060-8586, Japan*
[3] *Division of General Dentistry Center for Dental Clinics, Hokkaido University Hospital, N14 W5, Kita-ku, Sapporo, Hokkaido 060-8648, Japan*
[4] *Department of Biomedical, Dental Materials and Engineering, Faculty of Dental Medicine, Hokkaido University, N13 W7, Kita-ku, Sapporo, Hokkaido 060-8586, Japan*
Corresponding author, Hirofumi MIYAJI; E-mail: miyaji@den.hokudai.ac.jp

Surface pre-reacted glass-ionomer (S-PRG) filler releases several ions, such as fluoride, borate and strontium ions, to exert bioactive effects. We fabricated an endodontic root canal sealer containing S-PRG fillers (S-PRG sealer) and then evaluated the antibacterial and anti-inflammatory properties of S-PRG sealer compared with sealer containing conventional silica fillers (silica sealer). Antibacterial tests showed that S-PRG sealer significantly reduced the turbidity of *Enterococcus faecalis* compared with silica sealer. Implantation of S-PRG or silica sealer blocks in rat subcutaneous tissue showed that S-PRG sealer decreased the proinflammatory response compared with silica sealer at 10 days post-implantation. In addition, immunostaining revealed that infiltration of CD68- and peroxidase-positive cells around the S-PRG sealer was significantly lower than that in silica sealer. Therefore, it was suggested that S-PRG sealer exhibits antibacterial and anti-inflammatory effects.

Keywords: *Enterococcus faecalis*, Inflammatory response, Surface pre-reacted glass-ionomer (S-PRG) filler, Rat subcutaneous tissue

INTRODUCTION

Endodontic root canal sealers play an important role in apical sealing in combination with a master gutta-percha point in the root canal filling procedure. Many types of endodontic sealers, such as those composed of zinc oxide (ZO)[1)], calcium hydroxide[2)], mineral trioxide aggregate[3)] and epoxy resin[4)], have been applied for clinical endodontic therapy. To enhance the success rate of endodontic therapy, the antibacterial property and biocompatibility of root canal sealers should be improved, as well as sealing ability and physical property. Residual bacteria in the root canal may cause reinfection, subsequently requiring retreatment. In addition, it is considered that endodontic sealers directly attach to periapical periodontal tissue at the apical foramen after root canal filling. Hence, unfavorable wound healing would be induced using a sealer with low biocompatibility.

Recently, an ion-releasing glass filler, surface pre-reacted glass-ionomer (S-PRG) filler, has been applied for dental treatment[5)]. S-PRG fillers exhibit many bioactivities, such as demineralization prevention[6,7)], tooth remineralization[8-10)], acid buffer capacity[11)] and antibacterial effects[12-14)], *via* release of six ions (fluoride, sodium, strontium, aluminum, silicate and borate). Fluoride and borate ions are well-known antibacterial and biopromotive substances. Fluoride-coated titanium can effectively inhibit the initial adhesion and colonization of bacterial cells[15)]. Furthermore, fluoride ion application to a wound dressing remarkably reduces bacterial growth and promotes cell proliferation[16)]. In addition, bioactive glass including borate is more resistant to *Escherichia coli* than silica-based glass[17)]. Antibacterial effects of fluoride and borate were reported to promote wound healing as a secondary effect[18,19)]. Therefore, we speculated that a root canal sealer containing S-PRG fillers might enhance periapical periodontal tissue healing through antibacterial effects by ion release.

In this study, ZO-based sealers containing S-PRG fillers (S-PRG sealer) or conventional silica fillers (silica sealer) were assessed for biosafety. A previous *in vitro* report revealed the long-term ion-releasing profiles of S-PRG sealer[20)]. Hence, we speculated that antibacterial effects of S-PRG sealer would be superior to those of silica sealer. However, materials containing antibacterial property generally exhibit low biocompatibility. Accordingly, we characterized the antibacterial property and cytocompatibility of S-PRG and silica sealers. In addition, tissue responses to S-PRG sealer implanted into rat subcutaneous tissue were histologically compared with those of silica sealer.

MATERIALS AND METHODS

Fabrication and characterization of S-PRG and silica sealers

S-PRG filler (average particle size: 3 μm) was fabricated as

Color figures can be viewed in the online issue, which is available at J-STAGE.

Received Feb 1, 2019: Accepted Apr 22, 2019
doi:10.4012/dmj.2019-029 JOI JST.JSTAGE/dmj/2019-029

described previously[5,10]. Frit of fluoroboroaluminosilicate glass (composition: 21.6 wt% SiO_2, 21.6 wt% Al_2O_3, 16.6 wt% B_2O_3, 27.2 wt% SrO, 2.6 wt% Na_2O and 10.4 wt% F) was produced by melting at 1,400°C for 2 h. After dry and wet grounding, the glass frit was treated with polysiloxane (SiO_2 content: 16 wt%; degree of condensation: 2–6) and aqueous treatment of polyacrylic acid (polymer content: 13.0 wt%, average molecular weight: 52,000) was subsequently manipulated to finally obtain S-PRG filler. Silica filler (Fuselex X, SiO_2 content: 98.5%, average particle size: 3 μm) was purchased from Tatsumori (Tokyo, Japan).

The components of S-PRG sealer and silica sealer are detailed in Tables 1 and 2, respectively. Silica sealer was prepared by replacing the total weight of S-PRG filler with silica filler. To fabricate sealer blocks, a mold (5 mm diameter and 2 mm height) was filled with sealer after mixing. Thereafter, blocks were stored under 100% humidity at 37°C for 2 days to harden completely. Subsequently, sealer blocks were characterized by a scanning electron microscope (SEM; S-4000, Hitachi, Tokyo, Japan) and field emission scanning electron microscope (JSM-6500F, JEOL, Tokyo, Japan) equipped with an energy dispersive X-ray (EDX) spectrometer.

MC3T3-E1 cells (1×10^4 cells, RIKEN BioResource Center, Tsukuba, Japan) were seeded onto the sealer block and cultured under 5% CO_2 at 37°C in culture medium (MEM alpha, GlutaMAX-I, Thermo Fisher Scientific, Waltham, MA, USA) supplemented with 10% fetal bovine serum (Qualified FBS, Thermo Fisher Scientific) and 1% antibiotics (penicillin-streptomycin, Thermo Fisher Scientific). After 2-h incubation, samples were fixed in 2.5% glutaraldehyde in 0.1 M sodium cacodylate buffer (pH 7.4) and then dehydrated in increasing concentrations of ethanol. After Pt-Pd coating, samples were analyzed using SEM. Water-soluble tetrazolium salt-8 (WST-8) assay was carried out after incubation for 1 day using the Cell Counting Kit-8 (Dojindo Laboratories, Mashiki, Japan) following the manufacturer's instructions. The absorbance at 450 nm was measured on a microplate reader (ETY-300, Tokyo Sokki, Yokohama, Japan).

Sealer blocks were set into 48-well microplates and suspension of *Enterococcus faecalis* strain ATCC 29212 (final concentration: 4.5×10^7 colony-forming units (CFU)/mL) was seeded and incubated at 37°C for 24 h under anaerobic condition in brain heart infusion (BHI) broth (Pearlcore®, Eiken Chemical, Tokyo, Japan). After incubation, the turbidity of each suspension was measured using a turbidimeter (CO7500 Colourwave, Funakoshi, Tokyo, Japan) at an absorbance of 590 nm.

Histological examination of sealers implanted into rat subcutaneous tissue

In vivo experiments were performed in accordance with the institutional animal use and care regulations of Hokkaido University (approval number 13-122) and approved by the Animal Research Committee of Hokkaido University. Eleven 10-week-old male Wistar rats weighing 190–210 g were given general anesthesia by intraperitoneal injection of medetomidine hydrochloride (0.15 mg/mL; Domitor, Nippon Zenyaku Kogyo, Koriyama, Japan), midazolam (2 mg/mL; Dormicum, Astellas Pharma, Tokyo, Japan), butorphanol tartrate (2.5 mg/mL; Vetorphale, Meiji Seika Pharma, Tokyo, Japan) and local injection of 2% lidocaine hydrochloride with 1:80,000 epinephrine (Xylocaine Cartridge for Dental Use, Dentsply Sirona, Tokyo, Japan). After a skin incision was made, a sealer block was implanted into the subcutaneous tissue on the back of each rat. Each rat received one S-PRG sealer block and one silica sealer block. Skin flaps were sutured and tetracycline hydrochloride ointment (Achromycin Ointment, POLA Pharma, Tokyo, Japan) was applied to the wound.

Rats were euthanized using an overdose of sodium pentobarbital (2.0 mL/kg) at 10 days post-implantation. Some samples, including sealer and the surrounding soft tissue, were fixed in 10% buffered formalin, embedded in paraffin wax after removing sealer residue and cut into 5-μm sections. Sections were stained with hematoxylin-eosin and observed under light microscopy. The degree of tissue inflammation was assessed using three stained sections (magnification: 200×). Inflammatory cell infiltration was scored using a moderate scale ranging from 0 to 3 as follows: 0, normal tissue; 1, mild; 2, moderate; and 3, severe response[21].

For immunohistochemistry, samples were perfusion-fixed by 4% formaldehyde in 0.1 M phosphate buffer, immersed in 30% sucrose solution and then frozen in liquid nitrogen. Immunostaining of 16-μm-thick

Table 1 Composition of S-PRG filler-containing root canal sealer

Powder	Zinc oxide-based inorganic compound filler, S-PRG filler, additive
Liquid	Poly carboxylic acid derived, water, other

S-PRG: surface pre-reacted glass-ionomer

Table 2 Composition of silica filler-containing root canal sealer

Powder	Zinc oxide-based inorganic compound filler, silica filler, additive
Liquid	Poly carboxylic acid derived, water, other

sections was performed as described previously[22]. After permeabilization with 0.3% Triton X-100 and normal donkey serum, sections were incubated overnight with mouse anti-CD68 (1:100 dilution; Bio-Rad Laboratories, Hercules, CA, USA). Antigen-antibody reaction sites were detected by incubation with Cy3-labeled anti-mouse IgG (Jackson ImmunoResearch Labs, West Grove, PA, USA). Stained sections were observed under a confocal laser scanning microscope (Fluoview, Olympus, Tokyo, Japan). To detect granulocytes, some sections were incubated in 0.01 M Tris-HCl buffer (pH 7.6) containing 0.01% 3,3´-diaminobenzidine and 0.001% H_2O_2. Stained sections were observed under light microscopy. The intensity of immunostaining for CD-68 and peroxidase was measured using software (ImageJ 1.41, National Institutes of Health, Bethesda, MD, USA).

Biological characterization of S-PRG and silica fillers

To clarify the bioactivity of S-PRG and silica fillers, 20 μL of aqueous dispersions of S-PRG and silica fillers (1 wt%) were dispensed into wells of 96-well microplates. After drying for 24 h to fabricate a layer of filler, EDX analysis of S-PRG and silica filler layers was carried out. Thereafter, osteoblastic MC3T3-E1 cells (1×10^4 cells) were seeded onto the layers and incubated at 37°C with 5% CO_2 using culture medium supplemented with 10% fetal bovine serum and 1% antibiotics. The WST-8 assay was performed after 24-h incubation. The absorbance at 450 nm was measured on a microplate reader.

To assess antibacterial properties of S-PRG and silica fillers, 50 μL of filler dispersion (1 wt%) were dispensed into wells of 48-well microplates. After drying for 24 h, *E. faecalis* strain ATCC 29212 (final concentration: 4.5×10^7 CFU/mL) was seeded and incubated at 37°C for 24 h under anaerobic condition in BHI broth. After 24-h incubation, the turbidity of each suspension was measured using a turbidimeter at an absorbance of 590 nm.

Statistical analysis

Data are presented as the mean and standard deviation. Differences between groups were analyzed using Student's *t*-test. *p*-Values <0.05 were inferred as statistically significant. All statistical procedures were performed using SPSS 11.0 (IBM, Armonk, NY, USA).

RESULTS

Characterization of S-PRG and silica sealers

SEM observation showed that S-PRG and silica sealers were constructed by particle aggregation (Fig. 1A). EDX analysis revealed that S-PRG sealer contained elements F and Sr, which were not observed in silica sealer (Fig. 1B).

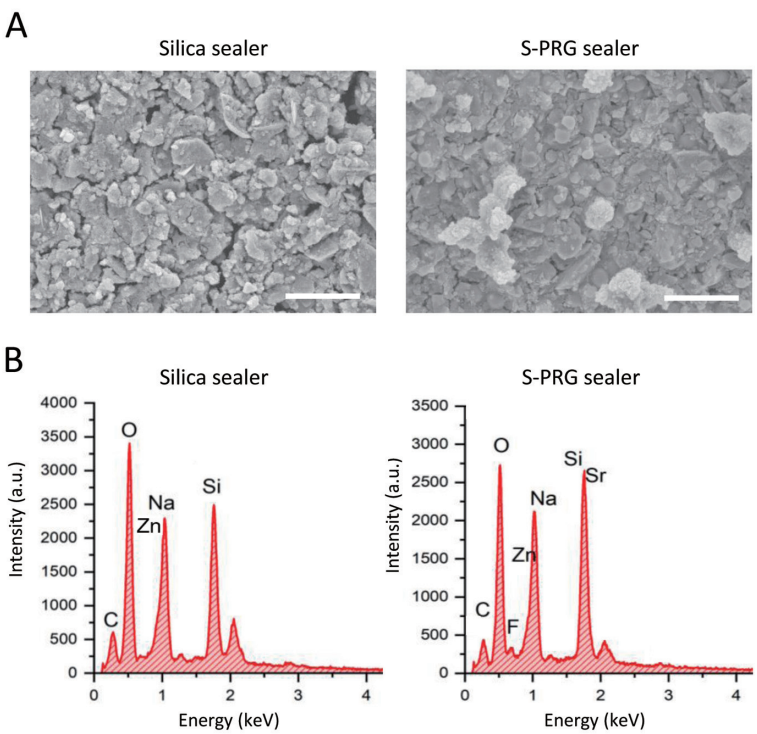

Fig. 1 Characterization of S-PRG and silica sealers.
(A) SEM micrographs of S-PRG and silica sealers. Scale bar represents 10 μm. (B) EDX analysis of S-PRG and silica sealers.
EDX, energy dispersive X-ray spectrometry; SEM, scanning electron microscopy; S-PRG, surface pre-reacted glass-ionomer.

To assess the cytocompatibility of the sealers, osteoblastic MC3T3-E1 cells were seeded onto S-PRG and silica sealer blocks. SEM images revealed that early cell attachment with cell spreading occurred on both sealers (Fig. 2A). In addition, WST-8 activity of 24-h cultured cells on sealer blocks was comparable between S-PRG and silica sealers (Fig. 2B). However, S-PRG sealer remarkably reduced the turbidity of *E. faecalis* compared with silica sealer ($p<0.01$, Fig. 2C).

Inflammatory response of rat subcutaneous tissue

At 10 days post-implantation, inflammatory cell aggregation was frequently observed in the connective tissue around the implanted silica sealer blocks. The silica sealer sample exhibited numerous blood vessels and lymphocyte-like cells in the connective tissue adjacent to the sealer block. However, inflammatory cell aggregation of the S-PRG sealer sample was relatively mild compared with that of the silica sealer sample. S-PRG sealer was encapsulated by dense connective tissue (Fig. 3). Mean inflammation scores of S-PRG and silica sealers at 10 days post-implantation were 1.0 and 1.5, respectively (Table 3).

Immunostaining of CD68 and peroxidase

Immunostaining revealed the accumulation of CD68-positive cells around the implanted sealers. The number of CD68-positive cells around S-PRG sealer was lower than that of silica sealer (Fig. 4A). The intensity of CD68 expression is shown in Fig. 4B. S-PRG sealer showed a significantly lower intensity of CD68 expression than that of silica sealer ($p<0.05$). In addition, peroxidase-positive granulocytes were sparsely detected around S-PRG sealer in contrast to silica sealers (Fig. 4C). The intensity of peroxidase expression of S-PRG sealer was significantly lower than that of silica sealer ($p<0.01$, Fig. 4D).

Characterization of S-PRG and silica fillers

EDX analysis showed that elements F, Na, Al, Si and Sr were detected in S-PRG filler. In contrast, silica filler mainly contained Si (Fig. 5A). To assess the cytocompatibility and antibacterial effect of S-PRG and silica fillers, culture tests were carried out. The results

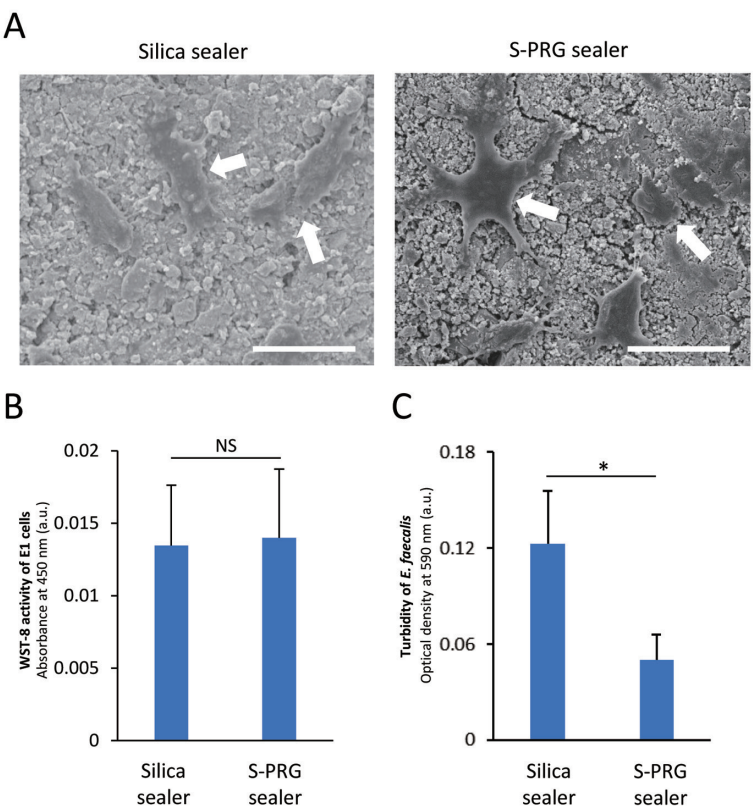

Fig. 2 Cytotoxic and antibacterial effects of S-PRG and silica sealers.
(A) SEM micrographs of MC3T3-E1 cells (white arrows) on S-PRG and silica sealers after 2-h incubation. Scale bar represents 30 μm. (B) WST-8 activity of MC3T3-E1 cells after 24-h incubation (n=6, mean±SD). (C) Turbidity of *Enterococcus faecalis* after 24-h incubation (n=5, mean±SD). *$p<0.01$.
SEM, scanning electron microscope; NS, not significant; SD, standard deviation; S-PRG, surface pre-reacted glass-ionomer; WST-8, water-soluble tetrazolium salt-8.

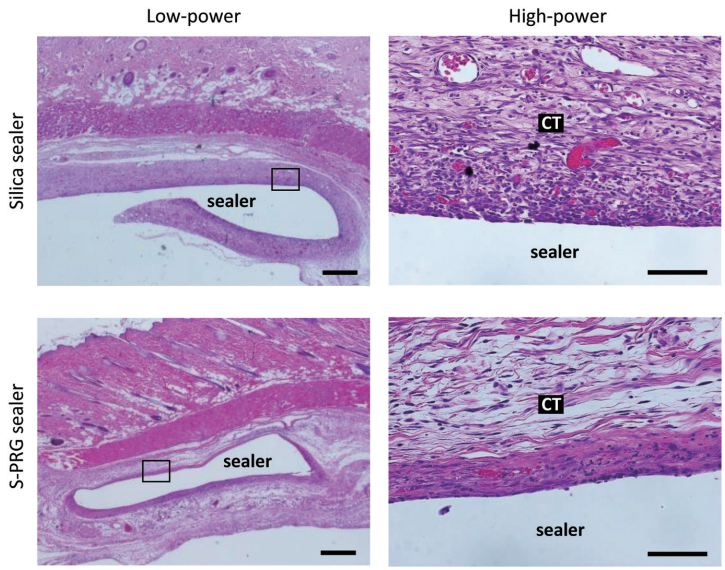

Fig. 3 Histological findings in subcutaneous tissue at 10 days post-implantation.
High-power images show the framed area in low-power images. Scale bar represents 1 mm in low-power images and 100 μm in high-power images. Hematoxylin-eosin staining.
CT, connective tissue; S-PRG, surface pre-reacted glass-ionomer.

Table 3 Inflammation scores at 10 days post-implantation (n=3, mean±standard deviation)

S-PRG sealer	1.0±0.0
Silica sealer	1.5±0.6

S-PRG: surface pre-reacted glass-ionomer

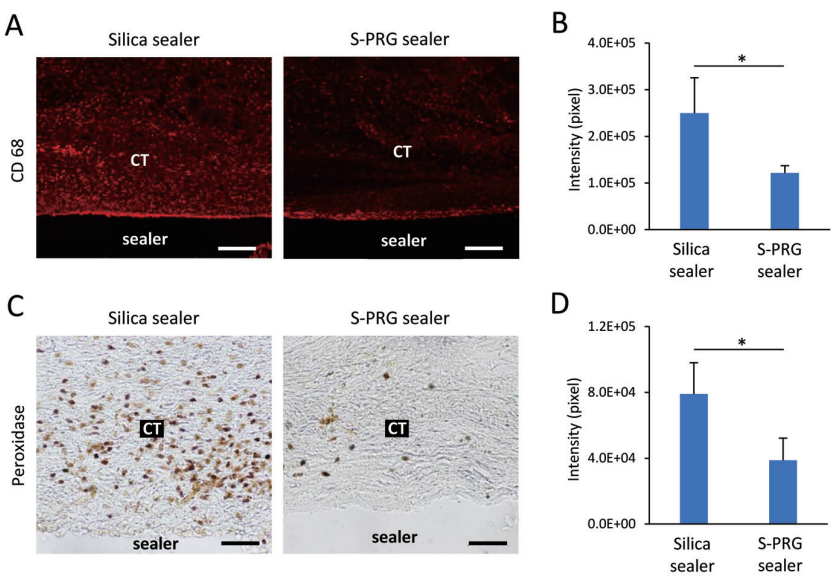

Fig. 4 Immunohistochemical assessments.
(A) Immunofluorescence micrographs of macrophages stained with mouse anti-CD68 (red). Scale bar represents 300 μm. (B) Intensity of CD68 expression (n=3, mean±SD). *p<0.05. (C) Peroxidase-stained (brown) micrographs of granulocytes. Scale bar represents 30 μm. (D) Intensity of peroxidase expression (n=5, mean±SD). *p<0.01.
CT, connective tissue; SD, standard deviation; S-PRG, surface pre-reacted glass-ionomer.

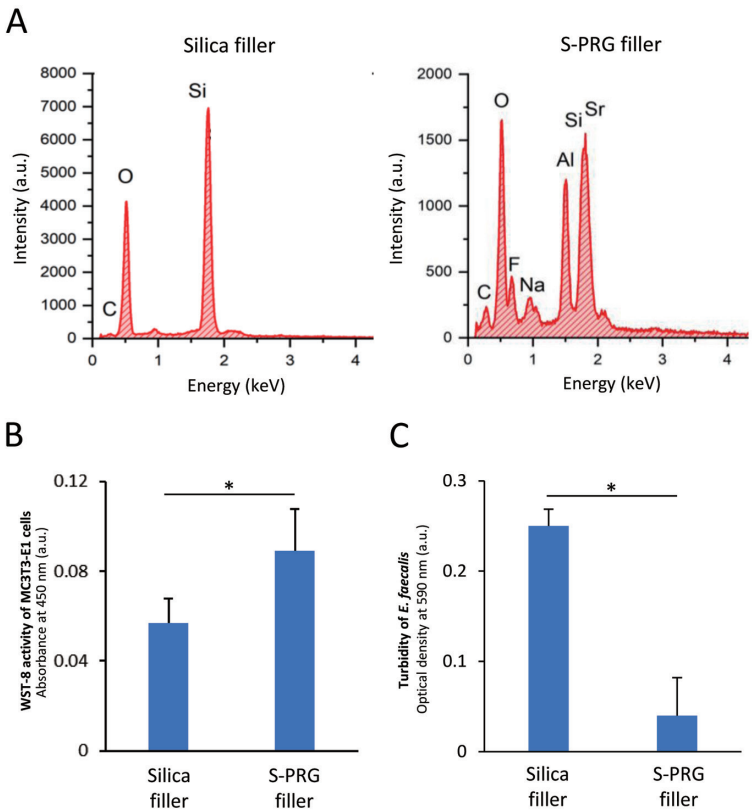

Fig. 5 Characterization of S-PRG and silica fillers.
(A) EDX analysis of S-PRG and silica fillers. (B) WST-8 activity of MC3T3-E1 cells after 24-h incubation (n=5, mean±SD). *p<0.05. (C) Turbidity of *E. faecalis* after 24-h incubation (n=5, mean±SD). *p<0.01.
EDX, energy dispersive X-ray spectrometry; S-PRG, surface pre-reacted glass-ionomer; WST-8, water-soluble tetrazolium salt-8.

of the WST-8 assay are shown in Fig. 5B. S-PRG filler significantly promoted WST-8 activity of MC3T3-E1 cells compared with silica filler (p<0.05). The results of turbidity of *E. faecalis* are shown in Fig. 5C. Turbidity of *E. faecalis* was significantly decreased by S-PRG filler application (p<0.01).

DISCUSSION

We considered from our results that the cytocompatibility of S-PRG and silica sealers was comparable. In contrast, S-PRG sealer diminished the turbidity of *E. faecalis* associated with the infected root canal[23], suggesting that S-PRG sealer possesses an antibacterial effect against *E. faecalis* (Fig. 2). Similar to S-PRG sealer, the layer of S-PRG filler exhibited a significant antibacterial effect against *E. faecalis* (Fig. 5C). Hence, it was considered that S-PRG filler contained in the sealer possesses antibacterial activity. Miki *et al.* previously assessed the antibacterial properties of resin containing S-PRG filler. They detected the release of antibacterial ions, such as fluoride, borate, aluminum and silicate, from resin containing S-PRG filler, and borate and fluoride ions, in particular, exhibited a great antiproliferative effect on *Streptococcus mutans*[24]. In addition, Kitagawa *et al.* reported that borate and fluoride ions released from S-PRG filler reduce *S. mutans* metabolism and acid production at a dose relatively lower than the growth inhibitory dose[25]. Fluoride ion directly acts as an inhibitor of glycolytic enzyme enolase and reduces the activity of acid resistance of bacteria[26]. Boron is associated with the inhibition of bacterial protein synthesis[27]. From the evidence of borate and fluoride ion release from S-PRG sealer[20], we speculated that the S-PRG filler-containing sealer sufficiently released antibacterial ions from S-PRG fillers to inhibit *E. faecalis* growth. S-PRG sealer would be biosafe and support endodontic healing as an antibacterial endodontic material.

In *in vivo* experiments, S-PRG sealer caused mild inflammatory cell infiltration, including CD68-positive macrophages and peroxidase-positive granulocytes, compared with silica sealer. Thus, it was considered that S-PRG sealer possesses mild proinflammatory properties. The anti-inflammatory effect of S-PRG sealer may be associated with the *in vivo* immune complex system related to ions released from S-PRG filler. Römer *et al.* reported that strontium ion enhances the proliferation of human periodontal ligament cells

and reduces interleukin (IL)-6 expression, suggesting that IL-6-induced inflammation would be suppressed[28]. Furthermore, strontium ion remarkably suppresses the amount of inflammatory substance, tumor necrosis factor α, secreted by macrophage-like cell line RAW264.7[29]. In addition to its effect on proinflammatory cytokine responses, strontium ion exhibits antioxidant activities. Jebahi *et al.* reported that strontium-doped bioglass reduces the generation of reactive oxygen species to promote soft tissue wound healing[30]. Borate ion also exhibits anti-inflammatory effects, similar to strontium ion. Ameen *et al.* reported that oral administration of borate dose-dependently decreases experimental chronic inflammation in rat[31]. They speculated that boron decreases the production of proinflammatory cytokines by monocytes/macrophages. Han *et al.* reported that strontium ion is also released from S-PRG sealer[20]. Hence, strontium and borate ions delivered from S-PRG sealer may downregulate inflammatory responses after root canal filling. Further investigation is needed to elucidate the detailed mechanisms of the anti-inflammatory effect of S-PRG sealer.

Interestingly, the S-PRG filler layer showed increased WST-8 activity compared with the silica filler layer. Hence, it was considered that some ions released from S-PRG filler might promote osteoblastic cell proliferation. Reportedly, strontium ion exhibits osteoinductive activities to promote bone healing. Strontium treatment facilitates proliferation and osteogenic differentiation of human adipose-derived stem cells[32] and collagen synthesis related to bone mineralization[33]. Furthermore, strontium increases expression of extracellular matrix genes and Wnt/catenin pathway genes to induce osteogenic differentiation of mesenchymal stem cells[34]. In addition, fluoride ion also increases osteoblast proliferation and expression of osseous markers and stimulates bone formation *in vivo*, similar to strontium ion[35,36]. Taken together, S-PRG filler may provide bioactive ions for increased osteogenesis of periodontal tissue after root canal filling. In vivo examination of the root canal filling model is needed to elucidate the cellular behavior of S-PRG sealer regarding apical periodontal tissue healing.

CONCLUSION

We herein assessed the antibacterial effects and cytocompatibility of S-PRG and silica sealers. Tissue compatibility of S-PRG and silica sealers was compared in rat subcutaneous tissue. S-PRG sealer inhibited *E. faecalis* growth compared with silica sealer. In addition, S-PRG sealer showed decreased aggregation of CD68- and peroxidase-positive cells to cause tissue inflammation compared with silica sealer. Therefore, S-PRG sealer may possess antibacterial and anti-inflammatory properties. S-PRG sealer is expected to be beneficial for periodontal soft tissue and alveolar bone healing after root canal filling.

ACKNOWLEDGMENTS

The authors acknowledge Prof. Toshihiko IWANAGA (Hokkaido University Faculty of Medicine) and Dr. Hiroko TAKITA (Hokkaido University Faculty of Dental Medicine) for their technical assistance. This work was supported by the MEXT Translational Research Network Program.

CONFLICT OF INTEREST

The authors report that they have no conflict of interest related to this study.

REFERENCES

1) Briseño B, Willershausen B. Root canal sealer cytotoxicity on human gingival fibroblasts. I. Zinc oxide-eugenol-based sealers. J Endod 1990; 16: 383-386.
2) Pitt Ford T, Rowe A. A new root canal sealer based on calcium hydroxide. J Endod 1989; 15: 286-289.
3) Thakur S, Emil J, Paulaian B. Evaluation of mineral trioxide aggregate as root canal sealer: A clinical study. J Conserv Dent 2013; 16: 494-498.
4) Zmener O, Spielberg C, Lamberghini F, Rucci M. Sealing properties of a new epoxy resin-based root-canal sealer. Int Endod J 1997; 30: 332-334.
5) Fujimoto Y, Iwasa M, Murayama R, Miyazaki M, Nagafuji A, Nakatsuka T. Detection of ions released from S-PRG fillers and their modulation effect. Dent Mater J 2010; 29: 392-397.
6) Ma S, Imazato S, Chen JH, Mayanagi G, Takahashi N, Ishimoto T, *et al.* Effects of a coating resin containing S-PRG filler to prevent demineralization of root surfaces. Dent Mater J 2012; 31: 909-915.
7) Murayama R, Furuichi T, Yokokawa M, Takahashi F, Kawamoto R, Takamizawa T, *et al.* Ultrasonic investigation of the effect of S-PRG filler-containing coating material on bovine tooth demineralization. Dent Mater J 2012; 31: 954-959.
8) Miyata S, Tanaka S, Matsuda Y, Hashimoto N, Sano H, Kawanami M. Caries prevention after surface reaction-type prereacted glass ionomer filler-containing coating resin removal from root surfaces. J Nanosci Nanotechnol 2016; 12: 12996-13000.
9) Shimazu K, Ogata K, Karibe H. Evaluation of the ion-releasing and recharging abilities of a resin-based fissure sealant containing S-PRG filler. Dent Mater J 2011; 30: 923-927.
10) Ito S, Iijima M, Hashimoto M, Tsukamoto N, Mizoguchi I, Saito T. Effects of surface pre-reacted glass-ionomer fillers on mineral induction by phosphoprotein. J Dent 2011; 39: 72-79.
11) Kaga M, Kakuda S, Ida Y, Toshima H, Hashimoto M, Endo K, *et al.* Inhibition of enamel demineralization by buffering effect of S-PRG filler-containing dental sealant. Eur J Oral Sci 2014; 122: 78-83.
12) Yoneda M, Suzuki N, Hirofuji T. Antibacterial effect of surface pre-reacted glass ionomer filler and eluate-mini review. Pharm Anal Acta 2015; 6: 349.
13) Saku S, Kotake H, Scougall-Vilchis RJ, Ohashi S, Hotta M, Horiuchi S, *et al.* Antibacterial activity of composite resin with glass-ionomer filler particles. Dent Mater J 2010; 29: 193-198.
14) Kimyai S, Lotfipour F, Pourabbas R, Sadr AO, Nikazar S, Milani MO. Effect of two prophylaxis methods on adherence of Streptococcus mutans to microfilled composite resin and giomer surfaces. Med Oral Patol Oral Cir Bucal 2011; 16:

561-567.
15) Liu H, Xiao J, Zhong W, Wang L, Qi M, Ying X, *et al.* In vitro behavior of bacteria on fluoride ion-coarted titanium: with special regands on Porphyromonas gingivalis. J Hard Tissue Biol 2011; 20: 47-52.
16) Seol-Ha J, Da-Yong S, In-Ku K, Eun-Ho S, Yun-Jeong S, Ji-Ung P, *et al.* Effective wound healing by antibacterial and bioactive calcium-fluoride-containing composite hydrogel dressings prepared using in situ precipitation. ACS Biomater Sci Eng 2018; 4: 2380-2389.
17) Rodriguez O, Stone W, Schemitsch EH, Zalzal P, Waldman S, Papini M, *et al.* Titanium addition influences antibacterial activity of bioactive glass coatings on metallic implants. Heliyon 2017; 3: e00420.
18) Bhawal UK, Lee HJ, Arikawa K, Shimosaka M, Suzuki M, Toyama T, *et al.* Micromolar sodium fluoride mediates anti-osteoclastogenesis in porphyromonas gingivalis-induced alveolar bone loss. Int J Oral Sci 2015; 7: 242-249.
19) Tepedelen BE, Soya E, Korkmaz M. Boric acid reduces the formation of DNA double strand breaks and accelerates wound healing process. Biol Trace Elem Res 2016; 174: 309-318.
20) Han L, Okiji T. Evaluation of the ions release/incorporation of the prototype S-PRG filler-containing endodontic sealer. Dent Mater J 2011; 30: 898-903.
21) Mori GG, de Moraes IG, Nunes DC, Castilho LR, Poi WR, Capaldi ML. Biocompatibility evaluation of alendronate paste in rat's subcutaneous tissue. Dent Traumatol 2009; 25: 209-212.
22) Nishida E, Miyaji H, Kato A, Takita H, Iwanaga T, Momose T, *et al.* Graphene oxide scaffold accelerates cellular proliferative response and alveolar bone healing of tooth extraction socket. Int J Nanomedine 2016; 11: 2265-2277.
23) Stuart CH, Schwartz SA, Beeson TJ, Owatz CB. Enterococcus faecalis: its role in root canal treatment failure and current concepts in retreatment. J Endod 2006; 32: 93-98.
24) Miki S, Kitagawa H, Kitagawa R, Kiba W, Hayashi M, Imazato S. Antibacterial activity of resin composites containing surface pre-reacted glass-ionomer (S-PRG) filler. Dent Mater 2016; 32: 1095-1102.
25) Kitagawa H, Miki-Oka S, Mayanagi G, Abiko Y, Takahashi N, Imazato S. Inhibitory effect of resin composite containing S-PRG filler on Streptococcus mutans glucose metabolism. J Dent 2018; 70: 92-96.
26) Marquis RE. Antimicrobial actions of fluoride for oral bacteria. Can J Microbiol 1995; 41: 955-964.
27) Uluisik I, Kaya A, Fomenko DE, Karakaya HC, Carlson BA, Gladyshev VN, *et al.* Boron stress activates the general amino acid control mechanism and inhibits protein synthesis. PLoS One 2011; 6: e27772.
28) Römer P, Desaga B, Proff P, Faltermeier A, Reicheneder C. Strontium promotes cell proliferation and suppresses IL-6 expression in human PDL cells. Ann Anat 2012; 194: 208-211.
29) Huang C, Li L, Yu X, Gu Z, Zhang X. The inhibitory effect of strontium-doped calcium polyphosphate particles on cytokines from macrophages and osteoblasts leading to aseptic loosening in vitro. Biomed Mater 2014; 9: 025010.
30) Jebahi S, Oudadesse H, Jardak N, Khayat I, Keskes H, Khabir A, *et al.* Biological therapy of strontium-substituted bioglass for soft tissue wound-healing: responses to oxidative stress in ovariectomised rats. Ann Pharm Fr 2013; 71: 234-242.
31) Ameen HNM, Hussain SA, Ahmed ZA, Aziz TA. Anti-inflammatory effects of boron alone or as adjuvant with dexamethasone in animal models of chronic and granulomatous inflammation. Int J Basic Clin Pharmacol 2015; 4: 701-707.
32) Nardone V, Zonefrati R, Mavilia C, Romagnoli C, Ciuffi S, Fabbri S, *et al.* In Vitro Effects of strontium on proliferation and osteoinduction of human preadipocytes. Stem Cells Int 2015; 2015: 871863.
33) Barbara A, Delannoya P, Denis BG. Marie PJ. Show more normal matrix mineralization induced by strontium ranelate in MC3T3-E1 osteogenic cells. Metabolism 2004; 53: 532-537.
34) Yang F, Yang D, Tu J, Zheng Q, Cai L, Wang L. Strontium enhances osteogenic differentiation of mesenchymal stem cells and in vivo boneformation by activating Wnt/catenin signaling. Stem Cells 2011; 29: 981-991.
35) Bellows CG, Heersche JN, Aubin JE. The effects of fluoride on osteoblast progenitors in vitro. J Bone Miner Res 1990; 5: 101-105.
36) Monjo M, Lamolle SF, Lyngstadaas SP, Rønold HJ, Ellingsen JE. In vivo expression of osteogenic markers and bone mineral density at the surface of fluoride-modified titanium implants. Biomaterials 2008; 29: 3771-3780.